Neurobiology of Disease 130 (2019) 104495

Contents lists available at ScienceDirect

Neurobiology of Disease

journal homepage: www.elsevier.com/locate/ynbdi

Neuroprotective effect of CuATSM on neurotoxin-induced motor neuron loss in an ALS mouse model

Michael T.H. Kuo[a,*], Joseph S. Beckman[e], Christopher A. Shaw[a,b,c,d]

[a] Department of Ophthalmology and Visual Sciences, University of British Columbia, Vancouver, British Columbia, Canada
[b] Department of Pathology, University of British Columbia, Vancouver, British Columbia, Canada
[c] Program in Neuroscience, University of British Columbia, Vancouver, British Columbia, Canada
[d] Program in Experimental Medicine, University of British Columbia, Vancouver, British Columbia, Canada
[e] Linus Pauling Institute, Department of Biochemistry and Biophysics, Oregon State University, Corvallis, OR, United States

ARTICLE INFO

Keywords:
Amyotrophic lateral sclerosis
ALS
CuATSM
Copper homeostasis
Neurodegeneration
Therapeutics

ABSTRACT

CuATSM is a PET-imaging agent that has recently received attention for its success in extending the lifespan in animals in several neurodegenerative disease models. In the SOD1^{G93A} model of ALS, CuATSM prolonged mouse longevity far longer than any previously tested therapeutic agents. The mechanism underlying this outcome has not been fully understood, but studies suggest that this copper complex contributes to maintaining copper homeostasis in mitochondria. More specifically for the SOD1 model, the molecule supplies copper back to the SOD1 protein. Additionally, CuATSM demonstrated similar protective effects in various *in vivo* Parkinson's disease mouse models. In the current pilot study, we utilized a neurodegenerative mouse model of motor neuron degeneration induced by the neurotoxin β-sitosterol β-D-glucoside. In this model, slow but distinct and progressive features of sporadic ALS occur. Treatment with CuATSM kept animal behavioural performance on par with the controls and prevented the extensive motor neuron degeneration and microglia activation seen in the untreated animals. These outcomes support a broader neuroprotective role for CuATSM beyond mutant SOD models of ALS.

1. Introduction

Amyotrophic lateral sclerosis (ALS) is a neurodegenerative disease characterized by motor neuron loss and the subsequent loss of motor function. Approximately 10% of all ALS cases are familial (fALS), defined by a Mendelian pattern of inheritance of at least 13 genes and loci. The remaining 90% are sporadic (sALS) where the causes remain elusive. For decades, the only effective therapeutic for ALS was riluzole whose effects are marginal. In the last 20 years, over 60 therapeutic compounds have failed to demonstrate clinical efficacy in human clinical trials (Petrov et al., 2017). Recently, Radicava (edaravone, a radical scavenger) has been approved. However, randomized control trials demonstrated efficacy only in early-stage patients, in concomitant use with riluzole, and that drug safety in patients with severe renal impairment, end-stage renal disease, or moderate-to-severe hepatic impairment remains to be evaluated (Sawada, 2017; Cruz, 2018). It is clear that the search to treat ALS is a long and arduous process, and what is currently accessible by patients has very limited efficacy.

The toxic gain-of-function mutations in the SOD1 (Cu/Zn superoxide dismutase type-1) gene have been most extensively studied in the various ALS models. The exact mechanisms for which SOD1 mutations contribute to disease progression are uncertain.

The normal SOD1 protein scavenges superoxide radicals by converting them to molecular oxygen and hydrogen peroxide (Fukai and Ushio-Fukai, 2011; Sea et al., 2015). To function properly in homodimer form, the SOD1 protein must undergo correct folding and maturation processes, requiring selective binding of copper and zinc ions for stabilizing and dimerizing (Kayatekin et al., 2008). The mutant SOD1, SOD1^{G93A}, retains the enzymatic activity only in the matured homodimer form (Khare et al., 2004; Rakhit et al., 2004; Ezzi et al., 2007; Wilcox et al., 2009), but does not bind copper ions as effectively as wild-type SOD1 (Pratt et al., 2014). The presence of increased expression of Copper-Chaperone-for-SOD (CCS), a metalloprotein that inserts copper ions into SOD1 and facilitates the maturation of SOD1 (Fukai and Ushio-Fukai, 2011), reduces the mean survival of SOD1^{G93A} mice eight fold (Son et al., 2007). The mechanisms behind CCS accelerating toxicity of SOD1^{G93A} have received attention because ALS patients express endogenous CCS in a much higher ratio to SOD compared

* Corresponding author.
E-mail address: michael.kuo@ubc.ca (M.T.H. Kuo).

https://doi.org/10.1016/j.nbd.2019.104495
Received 28 February 2019; Received in revised form 27 May 2019; Accepted 5 June 2019
Available online 07 June 2019
0969-9961/ © 2019 Elsevier Inc. All rights reserved.

to the ratio of endogenous CCS in $SOD1^{G93A}$ models (Rothstein et al., 1999). Several studies show that when human CCS (87% protein homology as mouse CCS) is co-expressed in low-expressing $SOD1^{G93A}$ mice, copper-dependent cytochrome *c* oxidase activity is greatly reduced in the spinal cord, demonstrating an apparent copper deficiency within the spinal cord. These animals die at up to eight times faster rate than those without human CCS (Son et al., 2008). These results suggest overexpression of CCS impairs copper-import into mitochondria by creating a copper deficit in prioritizing copper to SOD1 (Son et al., 2007; Son and Elliott, 2014).

To further explore a role for copper homeostasis in ALS, recent studies investigated a copper complex diacetylbis(N(4)-methylthiosemicarbazonato) copper(II) (CuATSM), which is capable of selectively releasing copper in cells with an impaired mitochondrial electron transport chain (Donnelly et al., 2012; Yoshii et al., 2012). At different dosages and methods of application, CuATSM was found to extend mean survival of high-expressing $SOD1^{G93A}$ mice by 16% (topical application, from an average 133 days to 155 days), up to 25% when treatment started as early as 5 days old (Williams et al., 2016), and low-expressing $SOD1^{G93A}$ mice by 15% (gavage, from an average 263 days to 300 days) (Soon et al., 2011). More impressively in double transgenic models, lifespan in high-expressing $SOD1^{G93A}$ × human CCS mice were extended by over 60-fold (topical, from 8 to 13 days to > 600 days) (Williams et al., 2016), and low-expressing SOD1G93A × human CCS mice by over 10-fold (topical, from 20 to 50 days to > 480 days) (Son et al., 2007; Williams et al., 2016).

CuATSM, a PET-imaging agent for hypoxic tumors in human (Dearling et al., 2002), is a neutral, lipophilic complex that readily crosses the blood-brain barrier (Fodero-Tavoletti et al., 2010). CuATSM also has a low reduction potential that facilitates a selective release of copper in cells with damaged mitochondria (Dearling and Packard, 2010; Donnelly et al., 2012; Yoshii et al., 2012). The unmetallated ATSM moiety has a high affinity for Cu^{2+} (Dearling and Packard, 2010). By itself, however, it was found to produce neither measurable improvement nor exacerbation of disease in the SOD1 mouse models (Vieira et al., 2017). But as CuATSM, it has consistently and independently demonstrated distinct rescue and neuroprotection properties in various mutant SOD1 mouse models, as cited above. The ALS rodent models used include a very aggressive variant of $SOD1^{G93A}$ model, in which the co-expression of copper chaperon CCS drastically shortens animal lifespan (Son et al., 2007; Son et al., 2008; Williams et al., 2016). While the mechanism for this acceleration is not fully understood, disrupted copper homeostasis in selective cells and the depletion of copper in the CNS were suggested as a major contributor to motor neuron death (Jonsson et al., 2006; Tokuda et al., 2007; Trumbull and Beckman, 2009; Tokuda et al., 2013). Additionally, CuATSM improved survival and locomotor functions in $SOD1^{G37R}$ model, in a dose-dependent manner (McAllum et al., 2013); compared to riluzole, which provided 3.3% increase on surivival, CuATSM at 60 mg/kg dosage yielded 26.3% improvement (McAllum et al., 2013). Mechanistically, CuATSM reportedly supplies copper to Cu-deficient SOD1 and converts it to holo-SOD1, thereby increasing the total SOD1 in $SOD1^{G37R}$ mice, but does not necessarily decrease misfolded SOD1 levels (Roberts et al., 2014). A decrease of misfolded SOD1 levels has been shown to improve the survival and locomotor function of mutant SOD1 mice (Gros-Louis et al., 2010; Liu et al., 2012). The lack of such decrease in the presence of CuATSM-mediated improvements in survival and locomotor function only adds to the unequivocal complexity of disease pathogenesis, suggesting only a partial contribution by the misfolded SOD1. Regardless, current studies of CuATSM in ALS mutant SOD1 models have all been very positive, and this is an exciting therapeutic potential for other neurodegenerative diseases such as copper-deficient SOD1 Parkinson's disease (PD) cases (Trist et al., 2017). This success has led to CuATSM being used in early clinical trial in human patients ("Phase 1 Dose Escalation and PK Study of Cu(II)ATSM in ALS/MND,", 2016). The results were favourable and encourages for further efforts on disease heterogeneity ("Theme 9 Clinical trials and trial design,", 2018). The Phase 2 trials of CuATSM will begin later 2019 in Sydney and Melbourne.

In addition to ALS, CuATSM has been shown effective in reversing parkinsonism defects in various disease models, both *in vitro* and *in vivo* (Hung et al., 2012). These models are thought to be unrelated to SOD protein activity. Peroxynitrite ($ONOO^-$) is formed from a non-enzymatic and pH-dependent reaction of nitric oxide and superoxide and is capable of modifying cellular activities, such as tyrosine nitration and lipid peroxidation (Beckman et al., 1990; Szabo et al., 2007). In context to PD, peroxynitrite induces nitration and aggregation of α-synuclein (Souza et al., 2000). Nitrated α-synuclein is neurotoxic, and the injection of this molecule into the *substantia nigra pars compacta* (SNpc) of rats produces many of the pathological features of PD (Yu et al., 2010).

Given CuATSM's success in these *in vivo* ALS and PD models, we sought to expand the previous studies that had employed mutant SOD1 (mSOD1) in fALS to include our own sporadic model of ALS. In the present study, we used a mouse model induced by an environmental neurotoxin, a dietary sterol glucoside β-sitosterol β-D-glucoside (BSSG), which produces features resembling the Guamanian variants of ALS and parkinsonism (ALS-parkinsonism dementia complex, ALS-PDC). Unlike the widely used transgenic ALS mouse models, our model shows a much slower onset of neural changes, but is progressive and provides well-defined sequential deficits that present in mice initially as motor neuron degeneration as seen in the classical ALS, sometimes followed later by basal ganglia defects, and lastly by deterioration in cortex and hippocampus, leading to cognitive decline (Wilson et al., 2002; Wilson and Shaw, 2007; Tabata et al., 2008).

2. Results

2.1. Physical and behavioural assessments

Weights were recorded weekly to monitor animal welfare and were found to be increasing normally per the Charles River datasheet. There were no significant differences between groups (Fig. 1A).

BSSG-fed animals exhibited a high degree of variance of the leg extension reflex from the beginning of testing, showing overall a consistent and significant decrease in the reflex ($p < .001$) compared to the controls and to the CuATSM-BSSG treated groups by week 32 (Fig. 1B).

BSSG-fed animals also showed a decrease in performance on the rotarod, with increasing variance between group mates that became significantly different from all other groups by 51 weeks of age. CuATSM treatment of BSSG-fed animals showed that that CuATSM maintained the treated animals near control levels (Fig. 1C).

2.2. Motor neuron counts

The motor neuron numbers in the lumbar spinal cord of BSSG-fed animals were significantly decreased, with some surviving motor neurons of these animals showing abnormal morphological features. Motor neurons in the BSSG group could show evidence of chromatolysis or pyknosis (Fig. 2B middle and right). BSSG-fed animals treated with CuATSM did not show the same loss of motor neurons or the morphological changes observed in the BSSG group. Averaged motor neuron counts revealed a 63% loss for the BSSG-fed animals compared to the control group. The CuATSM treatment group with BSSG fed mice mitigated this loss to 15% ($p < .001$) (Fig. 2C).

The DMSO (vehicle) group showed a 48% loss. DMSO is known to be neurotoxic ($p < .001$) (Fig. 2C). Treatment with CuATSM, however, similarly reduced the loss to 18% (Fig. 2C).

No significant differences in motor neuron loss were seen between right or left ventral horns (Fig. 2D).

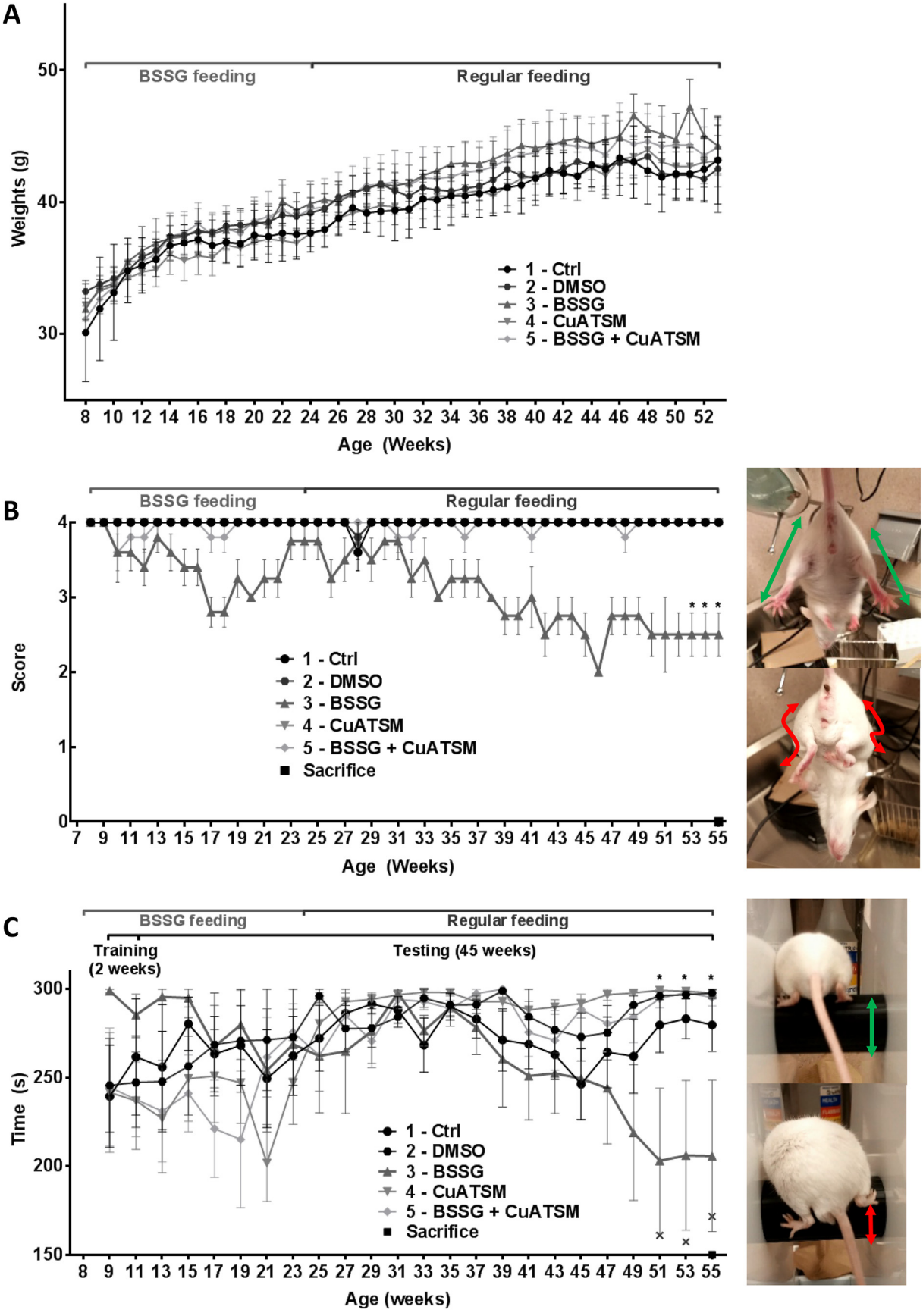

(caption on next page)

Fig. 1. Weights and motor assessments characterizing therapeutic effects of CuATSM on environmental toxin-induced sALS mouse modelusing BSSG, mean ± SEM. (A) Normal weight increase in accordance with vender Charles River datasheet, preventing reduced BSSG toxicity. (B) Left: Leg extension reflex on a 0–4 point scale; Right: Score 4 represents normal hind leg extension (Green arrows) and Score 2 represents failure to extend at least one hind leg (Red arrows) (* $p < .001$ to Ctrl and to BSSG + CuATSM groups; Two-way ANOVA followed by Tukey). (C) Left: Rotarod performance showing a declining progression in the BSSG-fed group while CuATSM treatment prevented such decline; Right: typical body stance of normal (Green arrow, seen in control and CuATSM-treated BSSG animals) *vs.* BSSG intoxicated animals were unable to keep pace with the speed of the Rotarod (Red arrow) (* $p < .05$ to Ctrl and to BSSG + CuATSM groups; Two-way ANOVA followed by Tukey). (For interpretation of the references to colour in this figure legend, the reader is referred to the web version of this article.)

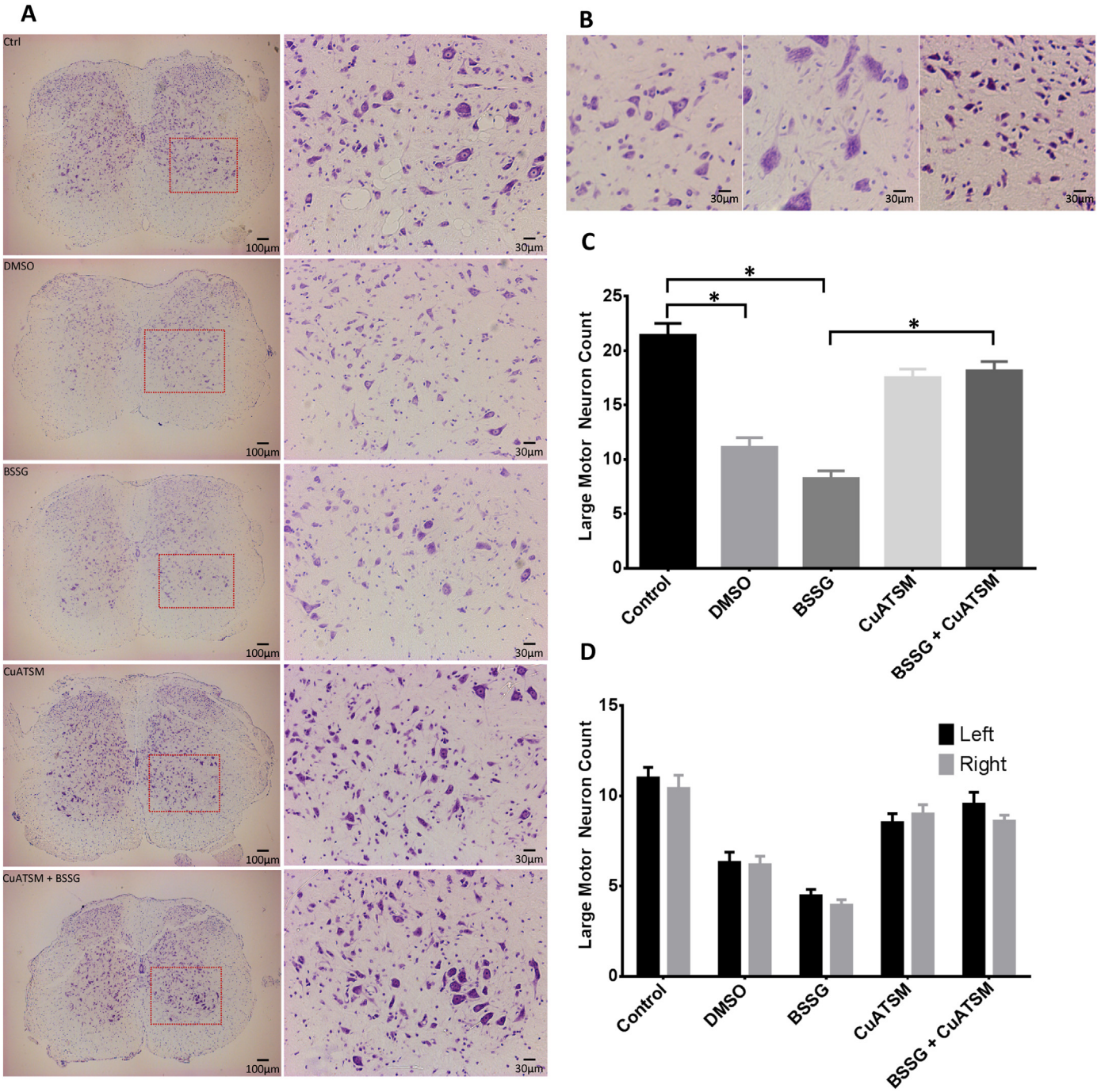

Fig. 2. Nissl staining and quantification of large motor neurons in ventral horn of lumbar (L2) spinal cord, mean ± SEM. (A) Representative micrographs from each group. (B) Morphological abnormalities found in BSSG-fed animals. Left, normal, taken from Control group. Middle, chromatolysis, characterized by swelling of cell body and dispersion of Nissl substance, taken from BSSG group. Right, pyknosis, characterized by chromatin condensation, and disappearance of Nissl substance, taken from BSSG group.(C) Averaged large motor neuron counts showing BSSG-fed animals treated with CuATSM were protected from motor neuron degeneration (* $p < .001$; One-way ANOVA followed by Tukey). (D) Averaged large motor neuron counts based on left or right ventral horn; difference did not reach statistical significance.

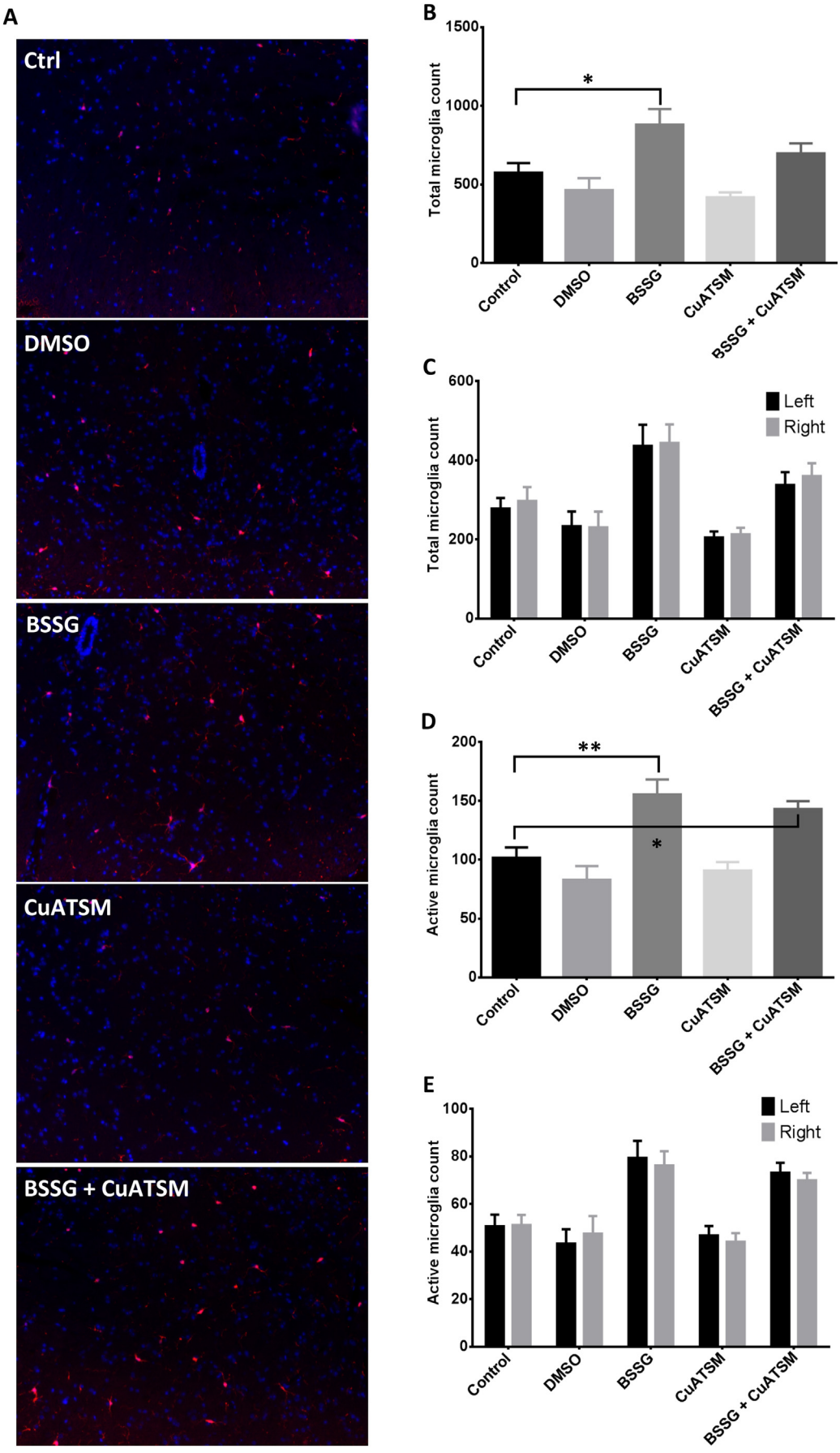

Fig. 3. Iba-1 immunolabelling and quantification of microglia in ventral horns of lumbar (L2) spinal cord, mean ± SEM. (A) Representative micrographs of microglia presence from each group. (B) Averaged total microglia counts showing significant increase in microglia levels in BSSG group compared to Control group and BSSG + CuATSM group to CuATSM group (* $p < .05$; One-way ANOVA followed by Tukey). (C) No statistical difference in total microglia counts between the left and right ventral horns. (D) Averaged activated microglia counts showing significant increase in activated microglia in BSSG group compared to Control group and BSSG + CuATSM group to CuATSM group (* $p < .05$, ** $p < .01$; One-way ANOVA followed by Tukey). (E) No statistical difference in activated microglia between the left and right ventral horns.

2.3. Activated microglia levels

BSSG-fed animals had an elevated level of total microglia of 53% more than controls ($p < .05$), and similarly for activated microglia as well (53%, $p < .01$) (Fig. 3B). CuATSM treatment in BSSG-fed animals, however, was able to restrict activated microglia increase to 41% (Fig. 3D, $p < .05$), while a 21% with total microglia that was not statistically significant (Fig. 3B).

Microglia of the DMSO (vehicle) group did not exhibit any significant change when compared to the control group.

3. Discussion

Our earlier work attempted to address a relative lack of sALS models by focusing on the Guamanian ALS variant whose expression was linked epidemiologically to consumption of seeds of a local variety of cycad (Borenstein et al., 2007). Our initial cycad characterization studies had identified several steryl glucosides found in cycad seeds as potential toxic principals that might be involved in ALS-PDC pathologies (Khabazian et al., 2002; Wilson et al., 2002; Tabata et al., 2008).

In this pilot study, we provide a preliminary assessment of CuATSM in our sALS model. BSSG-fed animals, as expected and consistent with previous studies as cited above, began to lose the leg extension reflex, a measure of α-motor neuron integrity, by 32 weeks of age. CuATSM treatment prevented the BSSG-induced loss of this reflex (Fig. 1B). Tests of motor function using the rotarod showed a similar preservation of function (Fig. 1C). CuATSM treatment substantially prevented typical forms of motor dysfunction, maintaining performance close to that of the control groups.

Histological analysis of the lumbar cord support these behavioural assessments indicated by the motor neuron degeneration in BSSG-fed animals and protection when treated with CuATSM. However, animals of the DMSO (vehicle) group exhibited a 48% loss of large motor neurons, while total microglia remained comparable to the control group (within 20%, not statistically significant). DMSO is a known neurotoxin with the potential to induce widespread apoptosis in the developing central nervous system in various animal models with extended exposure (Jacob and Rosenbaum, 1966; Castro et al., 1995; Hanslick et al., 2009; Galvao et al., 2014). We speculate that while DMSO toxicity caused fairly significant motor neuron loss, the surviving motor neurons were able to compensate by re-innervating the denervated muscles, a phenomenon that has been previously documented (Nijssen et al., 2017), whereas BSSG toxicity reduced more motor neurons and overwhelmed any compensating potentials by the surviving few motor neurons. In short, DMSO toxicity did not reduce motor neuron level below the “threshold” that would affect motor functions of the animals, and they were able to maintain their performance in behavioural assessments (Fig. 1B and C). It should be noted that CuATSM was able to mitigate damages caused by DMSO toxicity and motor neuron loss was prevented in the CuATSM group, where 100% DMSO was used as vehicle for delivery (Fig. 2C), which further reinforces the notion of neuroprotection by CuATSM.

Iba-1 labelling revealed a markedly elevated microglia level in the BSSG group (Fig. 3B). CuATSM treatment was able to lower this elevation, however, the difference between BSSG group and CuATSM-treated BSSG group did not reach significance, possibly due to the small sample size in the current experiments. Others have reported a reduced microglia presence in mutant SOD1 models (Soon et al., 2011; Roberts et al., 2014; Hilton et al., 2017). Interestingly, while motor neurons were reduced as a result of DMSO exposure in the DMSO group, microglia level remained comparable to the control group. It is possible that motor function impairment requires microglial activation as well as neuronal loss, and this will require time point analysis comparing early and late stages of the disease progression. Alternatively, the ability of CuATSM to prevent cellular degeneration may be specific to certain cell types. The proportion of activated microglia, algorithmically selected based on size and shape, was consistent in each group (Fig. 3D). The elevated microglia count supports a role of a general neuroinflammatory process in BSSG-induced neurotoxicity that is consistent with previous studies (Lee et al., 2007; Tabata et al., 2008).

Collectively, the findings reported in the current article support the notion of a general neuroprotection of motor neurons in an *in vivo* model of sporadic ALS by the copper compound, CuATSM. Taken together with the recently increasing positive reports of CuATSM as a potential therapeutic agents, a mitochondrial copper defect may be a key factor in some forms of neurodegenerative disorders (Trumbull and Beckman, 2009; Roberts et al., 2014; Williams et al., 2016; Hilton et al., 2017). Given these outcomes, it would seem worthwhile pursuing larger and more comprehensive *in vivo* studies to show that CuATSM has unequivocal therapeutic potential in the context of copper homeostasis, in ALS or other neurodegenerative disorders, thereby opening up new avenues for effective treatments. As there are currently no reliable biomarkers for early disease detection, it would be imperative to explore CuATSM neuroprotectivity after the BSSG toxins had a chance to reduce enough motor neurons to elicit clear locomotor deficits.

4. Material and methods

4.1. Animals

All animal procedures were conducted in compliance with the guidelines of the UBC Animal Care and Use Program (ACUP) and the Canadian Council on Animal Care (CCAC). The experimental protocol and animal welfare monitoring were examined and approved by the UBC Animal Care Committee (ACC).

Twenty-five male, CD-1 outbred mice were purchased from Charles River (Wilmington, MA, USA). CD-1 s were selected for this pilot study as they have been previously been successfully used in an our ALS-PDC model (Wilson et al., 2002; Wilson and Shaw, 2007; Tabata et al., 2008; Van Kampen et al., 2015). The animals were 8 weeks old upon arrival at our facility. After an additional one-week acclimatization period, the animals were randomly assigned to five groups, with five animals per group ($n = 5$): Control, DMSO (vehicle) Control, BSSG treatment, CuATSM treatment, and BSSG/CuATSM treatment.

As this was a pilot study designed to investigate potential therapeutic effects of CuATSM, the small n per group utilized was the minimum size to detect the presence of effect toxic and protective effects, while serving to approximate sample sizes for future studies.

The animals were housed singly to prevent conspecific aggression and more importantly, to ensure they consumed their designated amount of BSSG in pellets.

The facility was maintained at 22 °C in a 14/10 h light/dark cycle, as per ACUP guidelines.

4.2. Mice removed from trials

One mouse from the BSSG group died on week 14 of 46-week period due to large tumor mass in the abdomen that was apparent upon necropsy. One other mouse from the DMSO (vehicle) group was found dead overnight on week 42; the cause of death was not identified.

4.3. Treatments

4.3.1. β-sitosterol-β-d-glucoside

BSSG was synthesized and supplied by NeuroQuest Inc. (Halifax, NS, Canada) and Neurodyn Life Sciences Inc. (Charlottetown, PE, Canada), respectively. The product was tested for toxicity by the manufacturer with an in-house *in vitro* toxicity assay using NSC-34 cell line and met the standard of purity (> 95%) and potency for animal model research.

For animal consumption, BSSG was prepared in pellets per Neurodyn's BSSG Pellet Production protocol (LP-275 v1.0). The pellets

were made with amylase-free flour and banana flavouring, then shaped into 1-g pellets containing 1 mg BSSG or none for all non-BSSG groups. The flour was tested for amylase with EnzChek™ Ultra Amylase Assay Kit (Thermofisher, E33651). This step was crucial as amylase can cleave off the glucose moiety from BSSG, eliminating its neurotoxic potency (Khabazian et al., 2002). Fresh batches of pellets were made every two weeks.

For a 16-week period, five days per week, groups designated for BSSG consumption followed a feeding regimen described in Neurodyn BSSG Feeding protocol (BP-90 v1.3), where the animals were denied food sources overnight (5 pm to 9 am the following morning). This overnight fast, together with the addition of banana flavouring, served to promote complete consumption of the experimental pellets supplied in the morning. Once control or BSSG pellet were dispensed, and once the pellets were consumed, a regular food source (LabDiet 5015) was returned *ad libitum* until 5 pm.

4.3.2. Copper(II) complex of diacetylbis(4-methylthiosemicarbazone)

CuATSM was provided by the Beckman laboratory.

To prepare CuATSM for treatment at a stock concentration of 1.5 μg/μL, 1.5 g CuATSM in powder was added to a volumetric flask, brought to volume with 100 mL of dry pharmaceutical grade DMSO (VWR Canada, CA82021–452) and dissolved in a bath sonicator for 15 min (Williams et al., 2016). The solution was aliquoted and stored in a − 20 °C freezer until use.

For a 46-week period, five days per week, twice daily, groups designated for CuATSM treatment received 30 mg/kg body weight per day from the CuATSM stock. The animals were weighed daily and the average weight was used to determine future CuATSM dosages. The topical application was accomplished by streaking the CuATSM solution along the neck and back of the animal, against the fur coat direction, with a pipette. This direct skin contact allowed for maximum absorption, and the fur helped retaining the compound on the animal as they moved around the cage following treatment.

4.4. Behavioural assessments

The cage IDs were coded and cage locations were randomized by a technician of another laboratory before the assessments. Data were recorded under the coded IDs and were only decoded prior to analysis.

4.5. Leg extension reflex

For 46-week period, twice a week, the animals were assessed for any progressive loss of function as the normal leg extension reflex gradually deteriorated to tremor, and then to total retraction. The 5 point scale we used was modified from the traditional test (Barneoud and Curet, 1999) to quickly evaluate progression of motor dysfunction (Wilson et al., 2002; Tabata et al., 2008). In each trial, animals were lifted at the base of the tail and held head down, for a maximum of 5 s, to assess for the presence or degree of loss of this reflex. The scores were: (4) Complete extension of both legs (normal); (3) Two legs extended with some tremors and/or punching motion of one leg; (2) One leg extended and the other retracted, or tremors in both legs; (1) One leg retracted and tremors in the other leg; (0) Both legs retracted.

4.6. Rotarod

For a 46-week period, once every two weeks, the animals were assessed for general motor function (Gerlai et al., 1996; Gerlai and Roder, 1996) and motor learning (Welsh et al., 2005) with the rotarod (Med Associates Inc., ENV-576 M). The animals were trained for two weeks before the test period and the time that they could remain walking and eventually running on a rotating axle (3.6 cm diameter) without either falling or clenching onto the axle was measured. The axle speed of rotation accelerated from 4 RPM to 40 RPM in 300 s, the maximum allowed test time. A maximum of three trials were recorded per assessment per animal, where the third trial could be exempted if the animal performed adequately for the first two trials (> 250 s).

4.7. Tissue preparation, immunohistochemistry, and histology

At the end of the 46-week period (animal age: 55 weeks old), the animals were anaesthetized with isoflurane and perfused *via* cardiac puncture with chilled 0.1 M PBS (pH 7.4), followed by chilled 10% phosphate-buffered formalin. Fixed spinal cord was removed *via* laminectomy, and post-fixed by immersion in fixative for 24 h before paraffin embedding. Transverse sections (6 μm) were prepared on a rotary microtome (Leica RM2235).

4.8. Motor neurons

Deparaffinized sections were incubated with filtered 0.1% cresyl violet solution (VWR Canada, CAAAJ64318–09) at room temperature for 3 min, followed by a distilled water rinse, then differentiated in 95% ethyl alcohol with 2 to 3 drops of glacial acetic acid per 80 mL alcohol for 2 to 3 min, and finally checked under microscope for optimum contrast. Sections were mounted on glass slides with Permount™ (Fisher Sci, SP15–500).

Lumbar (L2) spinal cord, with 3 to 4 sections per animal that were 60 μm apart between sections in the rostral-caudal plane, were used for counting. Images were captured under bright-field (Olympus IX71) at 100 × magnification. Large motor neurons in the ventral horn regions (651 μm × 486 μm) were counted using ImageJ, algorithmically selecting for the appropriate size (> 220 μm^2), nucleus visibility, and intact cellular structures. Overlays of the selected cells were added to the original images and manually scanned to ensure the selections were not false- positive or negative picked up by ImageJ.

4.9. Microglia

Deparaffinized sections underwent antigen retrival using 10 mM sodium citrate with 0.05% Tween-20, at 90 °C for 50 min, washed with PBS for 3 × 10 min, blocked with 2% BSA in PBS with 0.2% Tween-20 (PBST), and incubated at 4 °C in 2% BSA in PBST containing the primary rabbit antibody for mouse Iba-1 (1:2000, Abcam, ab178846), overnight. Sections were then washed with PBST for 3 × 10 min, and incubated at room temperature in 1% BSA in PBST containing the secondary goat antibody Alexa 568 (1:300, Thermofisher, A11011), for 2 h. After another PBST wash 3 × 10 min, sections were incubated with DAPI (Thermofisher, D3571) in PBST, at room temperature for 10 min. The sections were mounted with Fluoromount™ (Sigma, F4680-25ML) after the final wash with PBS, 3 × 10 min.

Lumbar (L2) spinal cord, with 3 to 4 sections per animal that were 60 μm apart between sections in the rostral-caudal plane, were used for counting. Images were captured with fluorescence microscopy (Zeiss Axiovert 200 M) at 200 × magnification. Four images were obtained per section, with dimension 260 μm × 205 μm, centering on the central canal of the cord section. Combined, this gave a counting area of 520 μm × 410 μm for each section. Microglia in this counting area were counted using ImageJ, algorithmically selecting for sizes between 2 μm^2 to 100 μm^2. The “roundness”, a ratio of the minor and major axes of the shape, and “circularity”, a ratio where 0 indicates an increasingly elongated shape and 1 a perfect circle, were considered as parameters to select for microglia at different morphology. To be considered as activated microglia, the amoeboid morphology was defined as having “roundness” and “circularity” of 0.5 to 1. As with motor neurons, overlays on original images were scanned to ensure proper selection.

4.10. Statistical analysis

For behavioural experiments, individual measurements for each

animal were calculated as mean ± *SEM* for each group. For histology experiments, average counts were collected from the 4 sections for each animal, then calculated as mean ± *SEM* for each group. Each group contained 4 to 5 animals. The means were compared using an unpaired, two-tailed *t*-test or a one-way ANOVA. A *post hoc* Tukey's test was used to compare all means after ANOVA (GraphPad Prism 6).

Acknowledgement

We thank Neurodyn for synthesizing BSSG and providing technical support and members of Neural Dynamics Research Group for their kind advice on this project. We also thank Ingrid Barta at UBC Biomedical Research Center for tissue embedding. This work was supported by grant from Luther Allyn Shourds Dean estate.

References

Barneoud, P., Curet, O., 1999. Beneficial effects of lysine acetylsalicylate, a soluble salt of aspirin, on motor performance in a transgenic model of amyotrophic lateral sclerosis. Exp. Neurol. 155 (2), 243–251. https://doi.org/10.1006/exnr.1998.6984.

Beckman, J.S., Beckman, T.W., Chen, J., Marshall, P.A., Freeman, B.A., 1990. Apparent hydroxyl radical production by peroxynitrite: implications for endothelial injury from nitric oxide and superoxide. Proc. Natl. Acad. Sci. U. S. A. 87 (4), 1620–1624.

Borenstein, A.R., Mortimer, J.A., Schofield, E., Wu, Y., Salmon, D.P., Gamst, A., Olichney, J., Thal, L.J., Silbert, L., Kaye, J., Craig, U.L., Schellenberg, G.D., Galasko, D.R., 2007. Cycad exposure and risk of dementia, MCI, and PDC in the Chamorro population of Guam. Neurology 68 (21), 1764–1771. https://doi.org/10.1212/01.wnl.0000262027.31623.b2.

Castro, C.A., Hogan, J.B., Benson, K.A., Shehata, C.W., Landauer, M.R., 1995. Behavioral effects of vehicles: DMSO, ethanol, Tween-20, Tween-80, and emulphor-620. Pharmacol. Biochem. Behav. 50 (4), 521–526.

Cruz, M.P., 2018. Edaravone (radicava): a novel neuroprotective agent for the treatment of amyotrophic lateral sclerosis. P T 43 (1), 25–28.

Dearling, J.L., Packard, A.B., 2010. Some thoughts on the mechanism of cellular trapping of Cu(II)-ATSM. Nucl. Med. Biol. 37 (3), 237–243. https://doi.org/10.1016/j.nucmedbio.2009.11.004.

Dearling, J.L., Lewis, J.S., Mullen, G.E., Welch, M.J., Blower, P.J., 2002. Copper bis (thiosemicarbazone) complexes as hypoxia imaging agents: structure-activity relationships. J. Biol. Inorg. Chem. 7 (3), 249–259. https://doi.org/10.1007/s007750100291.

Donnelly, P.S., Liddell, J.R., Lim, S., Paterson, B.M., Cater, M.A., Savva, M.S., Mot, A.I., James, J.L., Trounce, I.A., White, A.R., Crouch, P.J., 2012. An impaired mitochondrial electron transport chain increases retention of the hypoxia imaging agent diacetylbis(4-methylthiosemicarbazonato)copperII. Proc. Natl. Acad. Sci. U. S. A. 109 (1), 47–52. https://doi.org/10.1073/pnas.1116227108.

Ezzi, S.A., Urushitani, M., Julien, J.P., 2007. Wild-type superoxide dismutase acquires binding and toxic properties of ALS-linked mutant forms through oxidation. J. Neurochem. 102 (1), 170–178. https://doi.org/10.1111/j.1471-4159.2007.04531.x.

Fodero-Tavoletti, M.T., Villemagne, V.L., Paterson, B.M., White, A.R., Li, Q.X., Camakaris, J., O'Keefe, G., Cappai, R., Barnham, K.J., Donnelly, P.S., 2010. Bis(thiosemicarbazonato) cu-64 complexes for positron emission tomography imaging of Alzheimer's disease. J. Alzheimers Dis. 20 (1), 49–55. https://doi.org/10.3233/JAD-2010-1359.

Fukai, T., Ushio-Fukai, M., 2011. Superoxide dismutases: role in redox signaling, vascular function, and diseases. Antioxid. Redox Signal. 15 (6), 1583–1606. https://doi.org/10.1089/ars.2011.3999.

Galvao, J., Davis, B., Tilley, M., Normando, E., Duchen, M.R., Cordeiro, M.F., 2014. Unexpected low-dose toxicity of the universal solvent DMSO. FASEB J. 28 (3), 1317–1330. https://doi.org/10.1096/fj.13-235440.

Gerlai, R., Roder, J., 1996. Spatial and nonspatial learning in mice: effects of S100 beta overexpression and age. Neurobiol. Learn. Mem. 66 (2), 143–154. https://doi.org/10.1006/nlme.1996.0055.

Gerlai, R., Millen, K.J., Herrup, K., Fabien, K., Joyner, A.L., Roder, J., 1996. Impaired motor learning performance in cerebellar En-2 mutant mice. Behav. Neurosci. 110 (1), 126–133.

Gros-Louis, F., Soucy, G., Lariviere, R., Julien, J.P., 2010. Intracerebroventricular infusion of monoclonal antibody or its derived fab fragment against misfolded forms of SOD1 mutant delays mortality in a mouse model of ALS. J. Neurochem. 113 (5), 1188–1199. https://doi.org/10.1111/j.1471-4159.2010.06683.x.

Hanslick, J.L., Lau, K., Noguchi, K.K., Olney, J.W., Zorumski, C.F., Mennerick, S., Farber, N.B., 2009. Dimethyl sulfoxide (DMSO) produces widespread apoptosis in the developing central nervous system. Neurobiol. Dis. 34 (1), 1–10. https://doi.org/10.1016/j.nbd.2008.11.006.

Hilton, J.B., Mercer, S.W., Lim, N.K., Faux, N.G., Buncic, G., Beckman, J.S., Roberts, B.R., Donnelly, P.S., White, A.R., Crouch, P.J., 2017. Cu(II)(atsm) improves the neurological phenotype and survival of SOD1(G93A) mice and selectively increases enzymatically active SOD1 in the spinal cord. Sci. Rep. 7, 42292. https://doi.org/10.1038/srep42292.

Hung, L.W., Villemagne, V.L., Cheng, L., Sherratt, N.A., Ayton, S., White, A.R., Crouch, P.J., Lim, S., Leong, S.L., Wilkins, S., George, J., Roberts, B.R., Pham, C.L., Liu, X., Chiu, F.C., Shackleford, D.M., Powell, A.K., Masters, C.L., Bush, A.I., O'Keefe, G., Culvenor, J.G., Cappai, R., Cherny, R.A., Donnelly, P.S., Hill, A.F., Finkelstein, D.I., Barnham, K.J., 2012. The hypoxia imaging agent CuII(atsm) is neuroprotective and improves motor and cognitive functions in multiple animal models of Parkinson's disease. J. Exp. Med. 209 (4), 837–854. https://doi.org/10.1084/jem.20112285.

Jacob, S.W., Rosenbaum, E.E., 1966. The toxicology of dimethyl sulfoxide (DMSO). Headache 6 (3), 127–136.

Jonsson, P.A., Graffmo, K.S., Andersen, P.M., Brannstrom, T., Lindberg, M., Oliveberg, M., Marklund, S.L., 2006. Disulphide-reduced superoxide dismutase-1 in CNS of transgenic amyotrophic lateral sclerosis models. Brain 129 (Pt 2), 451–464. https://doi.org/10.1093/brain/awh704.

Kayatekin, C., Zitzewitz, J.A., Matthews, C.R., 2008. Zinc binding modulates the entire folding free energy surface of human cu,Zn superoxide dismutase. J. Mol. Biol. 384 (2), 540–555. https://doi.org/10.1016/j.jmb.2008.09.045.

Khabazian, I., Bains, J.S., Williams, D.E., Cheung, J., Wilson, J.M., Pasqualotto, B.A., Pelech, S.L., Andersen, R.J., Wang, Y.T., Liu, L., Nagai, A., Kim, S.U., Craig, U.K., Shaw, C.A., 2002. Isolation of various forms of sterol beta-D-glucoside from the seed of Cycas circinalis: neurotoxicity and implications for ALS-parkinsonism dementia complex. J. Neurochem. 82 (3), 516–528.

Khare, S.D., Caplow, M., Dokholyan, N.V., 2004. The rate and equilibrium constants for a multistep reaction sequence for the aggregation of superoxide dismutase in amyotrophic lateral sclerosis. Proc. Natl. Acad. Sci. U. S. A. 101 (42), 15094–15099. https://doi.org/10.1073/pnas.0406650101.

Lee, G., Cruz-Aguado, R., Banjo, O.C., Shaw, C.A., 2007. Characterization of gait analysis, memory, and neuromuscular junction integrity in a mouse model of ALS-PDC. In: Paper presented at the Society for Neuroscience, San Diego, CA, USA, November 2017.

Liu, H.N., Tjostheim, S., Dasilva, K., Taylor, D., Zhao, B., Rakhit, R., Brown, M., Chakrabartty, A., McLaurin, J., Robertson, J., 2012. Targeting of monomer/misfolded SOD1 as a therapeutic strategy for amyotrophic lateral sclerosis. J. Neurosci. 32 (26), 8791–8799. https://doi.org/10.1523/JNEUROSCI.5053-11.2012.

McAllum, E.J., Lim, N.K., Hickey, J.L., Paterson, B.M., Donnelly, P.S., Li, Q.X., Liddell, J.R., Barnham, K.J., White, A.R., Crouch, P.J., 2013. Therapeutic effects of CuII(atsm) in the SOD1-G37R mouse model of amyotrophic lateral sclerosis. Amyotroph Lateral Scler Frontotemporal Degener 14 (7–8), 586–590. https://doi.org/10.3109/21678421.2013.824000.

Nijssen, J., Comley, L.H., Hedlund, E., 2017. Motor neuron vulnerability and resistance in amyotrophic lateral sclerosis. Acta Neuropathol. 133 (6), 863–885. https://doi.org/10.1007/s00401-017-1708-8.

Petrov, D., Mansfield, C., Moussy, A., Hermine, O., 2017. ALS Clinical trials review: 20 years of failure. Are we any closer to registering a new treatment? Front. Aging Neurosci. 9, 68. https://doi.org/10.3389/fnagi.2017.00068.

Phase 1 Dose Escalation and PK Study of Cu(II)ATSM in ALS/MND, 2016. March 6, 2017 Retrieved from. https://clinicaltrials.gov/ct2/show/NCT02870634.

Pratt, A.J., Shin, D.S., Merz, G.E., Rambo, R.P., Lancaster, W.A., Dyer, K.N., Borbat, P.P., Poole II, F.L., Adams, M.W., Freed, J.H., Crane, B.R., Tainer, J.A., Getzoff, E.D., 2014. Aggregation propensities of superoxide dismutase G93 hotspot mutants mirror ALS clinical phenotypes. Proc. Natl. Acad. Sci. U. S. A. 111 (43), E4568–E4576. https://doi.org/10.1073/pnas.1308531111.

Rakhit, R., Crow, J.P., Lepock, J.R., Kondejewski, L.H., Cashman, N.R., Chakrabartty, A., 2004. Monomeric cu,Zn-superoxide dismutase is a common misfolding intermediate in the oxidation models of sporadic and familial amyotrophic lateral sclerosis. J. Biol. Chem. 279 (15), 15499–15504. https://doi.org/10.1074/jbc.M313295200.

Roberts, B.R., Lim, N.K., McAllum, E.J., Donnelly, P.S., Hare, D.J., Doble, P.A., Turner, B.J., Price, K.A., Lim, S.C., Paterson, B.M., Hickey, J.L., Rhoads, T.W., Williams, J.R., Kanninen, K.M., Hung, L.W., Liddell, J.R., Grubman, A., Monty, J.F., Llanos, R.M., Kramer, D.R., Mercer, J.F., Bush, A.I., Masters, C.L., Duce, J.A., Li, Q.X., Beckman, J.S., Barnham, K.J., White, A.R., Crouch, P.J., 2014. Oral treatment with cu(II)(atsm) increases mutant SOD1 in vivo but protects motor neurons and improves the phenotype of a transgenic mouse model of amyotrophic lateral sclerosis. J. Neurosci. 34 (23), 8021–8031. https://doi.org/10.1523/JNEUROSCI.4196-13.2014.

Rothstein, J.D., Dykes-Hoberg, M., Corson, L.B., Becker, M., Cleveland, D.W., Price, D.L., Culotta, V.C., Wong, P.C., 1999. The copper chaperone CCS is abundant in neurons and astrocytes in human and rodent brain. J. Neurochem. 72 (1), 422–429.

Sawada, H., 2017. Clinical efficacy of edaravone for the treatment of amyotrophic lateral sclerosis. Expert. Opin. Pharmacother. 18 (7), 735–738. https://doi.org/10.1080/14656566.2017.1319937.

Sea, K., Sohn, S.H., Durazo, A., Sheng, Y., Shaw, B.F., Cao, X., Taylor, A.B., Whitson, L.J., Holloway, S.P., Hart, P.J., Cabelli, D.E., Gralla, E.B., Valentine, J.S., 2015. Insights into the role of the unusual disulfide bond in copper-zinc superoxide dismutase. J. Biol. Chem. 290 (4), 2405–2418. https://doi.org/10.1074/jbc.M114.588798.

Son, M., Elliott, J.L., 2014. Mitochondrial defects in transgenic mice expressing cu,Zn superoxide dismutase mutations: the role of copper chaperone for SOD1. J. Neurol. Sci. 336 (1–2), 1–7. https://doi.org/10.1016/j.jns.2013.11.004.

Son, M., Puttaparthi, K., Kawamata, H., Rajendran, B., Boyer, P.J., Manfredi, G., Elliott, J.L., 2007. Overexpression of CCS in G93A-SOD1 mice leads to accelerated neurological deficits with severe mitochondrial pathology. Proc. Natl. Acad. Sci. U. S. A. 104 (14), 6072–6077. https://doi.org/10.1073/pnas.0610923104.

Son, M., Leary, S.C., Romain, N., Pierrel, F., Winge, D.R., Haller, R.G., Elliott, J.L., 2008. Isolated cytochrome c oxidase deficiency in G93A SOD1 mice overexpressing CCS protein. J. Biol. Chem. 283 (18), 12267–12275. https://doi.org/10.1074/jbc.M708523200.

Soon, C.P., Donnelly, P.S., Turner, B.J., Hung, L.W., Crouch, P.J., Sherratt, N.A., Tan, J.L., Lim, N.K., Lam, L., Bica, L., Lim, S., Hickey, J.L., Morizzi, J., Powell, A., Finkelstein, D.I., Culvenor, J.G., Masters, C.L., Duce, J., White, A.R., Barnham, K.J., Li, Q.X., 2011. Diacetylbis(N(4)-methylthiosemicarbazonato) copper(II) (CuII(atsm)) protects against peroxynitrite-induced nitrosative damage and prolongs survival in

amyotrophic lateral sclerosis mouse model. J. Biol. Chem. 286 (51), 44035–44044. https://doi.org/10.1074/jbc.M111.274407.

Souza, J.M., Giasson, B.I., Chen, Q., Lee, V.M., Ischiropoulos, H., 2000. Dityrosine cross-linking promotes formation of stable alpha -synuclein polymers. Implication of nitrative and oxidative stress in the pathogenesis of neurodegenerative synucleinopathies. J. Biol. Chem. 275 (24), 18344–18349. https://doi.org/10.1074/jbc.M000206200.

Szabo, C., Ischiropoulos, H., Radi, R., 2007. Peroxynitrite: biochemistry, pathophysiology and development of therapeutics. Nat. Rev. Drug Discov. 6 (8), 662–680. https://doi.org/10.1038/nrd2222.

Tabata, R.C., Wilson, J.M., Ly, P., Zwiegers, P., Kwok, D., Van Kampen, J.M., Cashman, N., Shaw, C.A., 2008. Chronic exposure to dietary sterol glucosides is neurotoxic to motor neurons and induces an ALS-PDC phenotype. NeuroMolecular Med. 10 (1), 24–39. https://doi.org/10.1007/s12017-007-8020-z.

Theme 9 Clinical trials and trial design, 2018. Amyotrophic Lateral Sclerosis and Frontotemporal Degeneration. 19(sup1). pp. 264–281. https://doi.org/10.1080/21678421.2018.1510576.

Tokuda, E., Ono, S., Ishige, K., Naganuma, A., Ito, Y., Suzuki, T., 2007. Metallothionein proteins expression, copper and zinc concentrations, and lipid peroxidation level in a rodent model for amyotrophic lateral sclerosis. Toxicology 229 (1–2), 33–41. https://doi.org/10.1016/j.tox.2006.09.011.

Tokuda, E., Okawa, E., Watanabe, S., Ono, S., Marklund, S.L., 2013. Dysregulation of intracellular copper homeostasis is common to transgenic mice expressing human mutant superoxide dismutase-1s regardless of their copper-binding abilities. Neurobiol. Dis. 54, 308–319. https://doi.org/10.1016/j.nbd.2013.01.001.

Trist, B.G., Davies, K.M., Cottam, V., Genoud, S., Ortega, R., Roudeau, S., Carmona, A., De Silva, K., Wasinger, V., Lewis, S.J.G., Sachdev, P., Smith, B., Troakes, C., Vance, C., Shaw, C., Al-Sarraj, S., Ball, H.J., Halliday, G.M., Hare, D.J., Double, K.L., 2017. Amyotrophic lateral sclerosis-like superoxide dismutase 1 proteinopathy is associated with neuronal loss in Parkinson's disease brain. Acta Neuropathol. 134 (1), 113–127. https://doi.org/10.1007/s00401-017-1726-6.

Trumbull, K.A., Beckman, J.S., 2009. A role for copper in the toxicity of zinc-deficient superoxide dismutase to motor neurons in amyotrophic lateral sclerosis. Antioxid. Redox Signal. 11 (7), 1627–1639. https://doi.org/10.1089/ARS.2009.2574.

Van Kampen, J.M., Baranowski, D.C., Robertson, H.A., Shaw, C.A., Kay, D.G., 2015. The progressive BSSG rat model of Parkinson's: recapitulating multiple key features of the human disease. PLoS One 10 (10), e0139694. https://doi.org/10.1371/journal.pone.0139694.

Vieira, F.G., Hatzipetros, T., Thompson, K., Moreno, A.J., Kidd, J.D., Tassinari, V.R., Levine, B., Perrin, S., Gill, A., 2017. CuATSM efficacy is independently replicated in a SOD1 mouse model of ALS while unmetallated ATSM therapy fails to reveal benefits. IBRO Rep 2, 47–53. https://doi.org/10.1016/j.ibror.2017.03.001.

Welsh, J.P., Yamaguchi, H., Zeng, X.H., Kojo, M., Nakada, Y., Takagi, A., Sugimori, M., Llinas, R.R., 2005. Normal motor learning during pharmacological prevention of Purkinje cell long-term depression. Proc. Natl. Acad. Sci. U. S. A. 102 (47), 17166–17171. https://doi.org/10.1073/pnas.0508191102.

Wilcox, K.C., Zhou, L., Jordon, J.K., Huang, Y., Yu, Y., Redler, R.L., Chen, X., Caplow, M., Dokholyan, N.V., 2009. Modifications of superoxide dismutase (SOD1) in human erythrocytes: a possible role in amyotrophic lateral sclerosis. J. Biol. Chem. 284 (20), 13940–13947. https://doi.org/10.1074/jbc.M809687200.

Williams, J.R., Trias, E., Beilby, P.R., Lopez, N.I., Labut, E.M., Bradford, C.S., Roberts, B.R., McAllum, E.J., Crouch, P.J., Rhoads, T.W., Pereira, C., Son, M., Elliott, J.L., Franco, M.C., Estevez, A.G., Barbeito, L., Beckman, J.S., 2016. Copper delivery to the CNS by CuATSM effectively treats motor neuron disease in SOD(G93A) mice co-expressing the copper-chaperone-for-SOD. Neurobiol. Dis. 89, 1–9. https://doi.org/10.1016/j.nbd.2016.01.020.

Wilson, J.M., Shaw, C.A., 2007. Late appearance of glutamate transporter defects in a murine model of ALS-parkinsonism dementia complex. Neurochem. Int. 50 (7–8), 1067–1077. https://doi.org/10.1016/j.neuint.2006.09.017.

Wilson, J.M., Khabazian, I., Wong, M.C., Seyedalikhani, A., Bains, J.S., Pasqualotto, B.A., Williams, D.E., Andersen, R.J., Simpson, R.J., Smith, R., Craig, U.K., Kurland, L.T., Shaw, C.A., 2002. Behavioral and neurological correlates of ALS-parkinsonism dementia complex in adult mice fed washed cycad flour. NeuroMolecular Med. 1 (3), 207–221. https://doi.org/10.1385/NMM:1:3:207.

Yoshii, Y., Yoneda, M., Ikawa, M., Furukawa, T., Kiyono, Y., Mori, T., Yoshii, H., Oyama, N., Okazawa, H., Saga, T., Fujibayashi, Y., 2012. Radiolabeled cu-ATSM as a novel indicator of overreduced intracellular state due to mitochondrial dysfunction: studies with mitochondrial DNA-less rho0 cells and cybrids carrying MELAS mitochondrial DNA mutation. Nucl. Med. Biol. 39 (2), 177–185. https://doi.org/10.1016/j.nucmedbio.2011.08.008.

Yu, Z., Xu, X., Xiang, Z., Zhou, J., Zhang, Z., Hu, C., He, C., 2010. Nitrated alpha-synuclein induces the loss of dopaminergic neurons in the substantia nigra of rats. PLoS One 5 (4), e9956. https://doi.org/10.1371/journal.pone.0009956.